SIMULATION OF PHYSICAL PROCESSES

Original article
DOI: https://doi.org/10.18721/JPM.15403

THE MULTICHARGED ION PLASMA UNDER EXTERNAL LASER PULSE: CALCULATION OF ITS KEY PARAMETERS

M. V. Timshina[1]✉, *N. V. Kalinin*[2]

[1] Ioffe Institute of the Russian Academy of Sciences, St. Petersburg, Russia;

[2] Peter the Great St. Petersburg Polytechnic University, St. Petersburg, Russia

✉ mariyatimshina@yandex.ru

Abstract. The paper presents a numerical study of laser radiation interaction with cylindrical plasma medium. The model has been described in detail. Non-equilibrium sodium ions were chosen as the active medium and a CO^2-laser as an external irradiator. The calculations used the one-dimensional two-temperature single-fluid radiative-hydrodynamic approximation taking into account the non-equilibrium ionic composition and the radiation absorption by plasma due to the inverse bremsstrahlung effect. In the calculations, the used laser pulse characteristics belonged to the range well-studied experimentally; e.g. the intensity of the incident laser radiation was about 100 TW/cm^2. The performed calculations were aimed at the development of research on the creation of active laser media based on the multicharged ions' transitions working in the extreme UV and soft X-ray bands.

Keywords: highly ionized plasma, radiation-hydrodynamic model, laser-plasma interaction

Funding: The reported study was funded by Russian Foundation for Basic Research according to the grant RFBR No. 20-38-90259.

Citation: Timshina M. V., Kalinin N. V., The multicharged ion plasma under external laser pulse: calculation of its key parameters, St. Petersburg State Polytechnical University Journal. Physics and Mathematics. 15 (4) (2022) 44–54. DOI: https://doi.org/10.18721/JPM.15403

Научная статья
УДК 533.9
DOI: https://doi.org/10.18721/JPM.15403

РАСЧЕТ КЛЮЧЕВЫХ ПАРАМЕТРОВ ПЛАЗМЫ МНОГОЗАРЯДНЫХ ИОНОВ ПРИ ВОЗДЕЙСТВИИ ВНЕШНЕГО ЛАЗЕРНОГО ИМПУЛЬСА

М. В. Тимшина[1]✉, *Н. В. Калинин*[2]

[1] Физико-технический институт им. А. Ф. Иоффе РАН, Санкт-Петербург, Россия;

[2] Санкт-Петербургский политехнический университет Петра Великого, Санкт-Петербург, Россия

✉ mariyatimshina@yandex.ru

Аннотация. Проведено численное исследование взаимодействия лазерного излучения с плазменной средой цилиндрической формы. В качестве среды рассмотрена плазма натрия, а внешнего облучателя – CO_2-лазер. В расчетах применялось одномерное двухтемпературное одножидкостное радиационно-гидродинамические приближение, учитывающее поглощение лазерного излучения плазмой за счет обратного тормозного эффекта и неравновесный ионный состав. Использованные характеристики лазерного импульса относятся к диапазону, хорошо освоенному экспериментально; например, его интенсивность составляла примерно 100 ТВт/см^2. Проведенные расчеты направлены на развитие исследований по созданию активных сред лазеров на переходах многозарядных ионов, работающих в экстремально ультрафиолетовом и мягком рентгеновском спектральных диапазонах.

Ключевые слова: плазма многозарядных ионов, радиационно-гидродинамическая модель, взаимодействие лазерного излучения с плазмой

Финансирование: Исследование выполнено при финансовой поддержке Российского фонда фундаментальных исследований (грант № 20-38-90259).

Для цитирования: Тимшина М. В., Калинин Н. В. Расчет ключевых параметров плазмы многозарядных ионов при воздействии внешнего лазерного импульса // Научно-технические ведомости СПбГПУ. Физико-математические науки. 2022. Т. 15. № 4. С. 44–54. DOI: https://doi.org/10.18721/JPM.15403

Introduction

As advances are made in infrared, visible and ultraviolet lasers, more studies emerge on devices generating in extreme ultraviolet and soft X-ray (EUV and SXR) ranges [1, 2]. Short-wave radiation in the EUV and SXR spectral ranges has a number of important advantages over radiation at longer wavelengths: it can be focused on a surface whose linear dimensions are of the order of laser radiation wavelength; this makes it possible to achieve a greater concentration of energy at shorter wavelengths. This shows great promise for high energy physics. In addition, EUV and SXR lasers offer high contrast and short pulse duration. Their brightness exceeds that of X-ray tubes by more than an order of magnitude, and is comparable to the brightness of synchrotron radiation. There are diverse applications for short-wave laser radiation in many fields of physics (for example, solid state physics and dense plasma physics), chemistry, biology and medicine. In particular, visualization of different types of nanostructures, e.g., cellular visualization [3–6] is especially interesting in the case of radiation at wavelengths below 10 nm.

There are two fundamentally different approaches to constructing short-wave radiation sources. The first one is based on converting (multiplying) the frequency of lasers generating in other spectral ranges by methods of nonlinear optics [7]. The other approach is aimed at generating radiation directly in the required short-wave range. Successful attempts have been made to construct free-electron lasers [8], allowing to generate X-ray pulses with record-high characteristics at unique large-scale facilities: the wavelengths can reach tenths of nanometers, and the radiation intensities 10^{30} photons/(s·mm^2·mrad^2). Efforts are also underway to create efficient and more compact short-wave lasers where the lasing medium is formed at the transitions of multicharged ions in highly ionized non-equilibrium plasma [9, 10]. High-current *Z*-discharges and high-power pulsed lasers are used to produce highly ionized plasma containing multicharged ions with the required isoelectronic sequence [11, 12]. Pulsed lasers are the preferred type, as they are the most powerful of the existing laboratory sources.

Description of the model

This paper specifically reports on modeling for the above approach to generating the gain medium in non-equilibrium multicharged ion plasma. Gaseous sodium was selected as the gain medium due to suitable electron transitions (≤10 nm) for hydrogen and helium-like ions:

radiation wavelength is 5.4 nm at $3\rightarrow2$ Na^{+10} transitions,

15.4 nm at $4\rightarrow3$ Na^{+10} transitions,

6.6 nm at $3\rightarrow2$ Na^{+9} transitions.

A CO_2 laser with a wavelength of 10.6 μm was taken as an external irradiator. Laser radiation fluxes to the lateral surface were limited to a level (comprehensively explored in experiments) not exceeding 100 TW/cm^2. The main mechanism of laser absorption in such fluxes is inverse bremsstrahlung [13]; for this reason, only this (classical) mechanism was taken into account in the model.

Several software packages are capable of simulating laser plasma of multicharged ions, for example, RADEX/LASNEX, HEIGHTS, RZLINE, RALEF, Z* [14–16]. These packages are intended for constructing laser-plasma point EUV radiation sources for microelectronics. It was by no means our intention to compete with such packages. Our main motivation to use our own program code was that we were thus capable of performing data-intensive computations for various experimental conditions, in order to find the optimal scenarios for constructing a laser source in the short-wave range.

We consider a cylindrically symmetric plasma target placed in vacuum, with a uniformly distributed flux of laser radiation falling on its surface. The physical processes evolving in the target plasma absorbing laser radiation are described by the equations of radiative magnetic gas dynamics (RMGD) in a two-temperature (2*T*) one-dimensional (1*D*) axisymmetric approximation.

The model takes into account the following physical phenomena:

non-stationary ionization,

energy exchange due to elastic collisions between electrons and heavy particles,

energy transfer due to thermal conductivity of electrons,

volumetric cooling of plasma by its self-emission in a continuous spectrum.

We consider laser radiation fluxes with an intensity $QL \leq 100$ TW/cm^2, at which parametric instabilities do not develop in the plasma so the role of radiation pressure can be neglected.

The corresponding system of 1D unsteady equations in terms of Lagrangian mass variables (1) consists of the equations for conservation of mass (2), momentum (3), energy (4), (5); the system takes the following form [17]:

$$\frac{dr}{dt} = u, \tag{1}$$

$$\frac{d}{dt}\left(\frac{1}{\rho}\right) = \frac{\partial}{\partial m}(ru), \tag{2}$$

$$\frac{du}{dt} = -r\frac{\partial}{\partial m}\left(P + P_{\omega}\right), \tag{3}$$

$$\frac{d}{dt}\left(E_e + E_{ion}\right) = -\left(P + P_{\omega}\right)\frac{\partial}{\partial m}\left(ru\right) - \frac{\partial W_e}{\partial m} - \frac{\partial W_L}{\partial m} - Q_{\Delta T} - Q_{rad}, \tag{4}$$

$$\frac{dE_i}{dt} = -P_i\frac{\partial}{\partial m}\left(ru\right) + Q_{\Delta T}, \tag{5}$$

$$W_e = -r^2\chi_0 T_e^{5/2}\rho\frac{\partial T_e}{\partial m}, \tag{6}$$

$$Q_{\Delta T} = C_0\rho^2\frac{T_i - T_e}{T_e^{3/2}}, \tag{7}$$

$$W_L = \frac{Q_L(t)}{2\pi}\left(e^{-(S-s)} - e^{-(S+s)}\right). \tag{8}$$

where t is the time; r is the Eulerian coordinate; m is the Lagrangian mass coordinate (the time derivatives are Lagrangian); u and ρ are the velocity and density of plasma; P_{ω} is the artificial viscosity; E_e, E_i are the specific internal energies of electrons and ions, respectively; E_{ion}, P_i, P_e are the specific ionization energy, the pressure of the ion and electron components, respectively ($P = P_i + P_e$); $Q_{\Delta T}$ is the energy exchange rate between ions and electrons during elastic interaction; W_e is the heat flux due to electron thermal conductivity; W_L is the laser radiation flux incident on the side surface of plasma bunch; η is the coefficient of laser radiation absorption by the target plasma; $Q_L(t)$ is the function determining the time variation of the laser radiation flux incident on the target; s is the instantaneous value of optical thickness, $s = \int_0^r \eta dr$; S is the total optical thickness of the plasma bunch, $S = \int_0^{R_{PL}(t)} \eta dr$ ($R_{pl}(t)$ is the radius of the moving plasma/vacuum interface); Q_{rad} is the specific power of the plasma self-emission.

We should note that

$$P_i = N_i T_i,\ P_e = N_e T_e,\ N_e = \overline{Z}N_i, \tag{9}$$

where N_i, N_e, T_i, T_e are the concentrations and temperatures of the ion and electron components, respectively; $\bar{z}$ is the mean ionic charge.

Non-equilibrium ionization was considered within the kinetic model using approximating interpolation coefficients of ionization and recombination. The equation determining the mean plasma charge follows the expression

$$\frac{dZ}{dt} = (V_{ion} - V_{thr} - V_{ph})Z, \tag{10}$$

where V_{ion} is the collisional ionization rate; V_{thr} is the triple recombination rate; V_{ph} is the photo-recombination rate [13, 18].

The degree to which the bunch is heated by the laser depends on the radiation flux incident on its surface.

The distribution of laser radiation fluxes propagating in the plasma towards the plasma bunch axis W_{L+} (with a plus sign) and in the opposite direction W_{L-} (with a minus sign) in the axisymmetric case is determined by the equation

$$\frac{\partial W_{L\pm}}{\partial m} = \pm \frac{W}{\rho r} \eta, \tag{11}$$

where η is the absorption coefficient of laser radiation.

These fluxes satisfy the symmetry conditions on the bunch axis; they are equal to the given laser radiation flux on its outer surface, so the function Q_L has the following form:

$$Q_L = \frac{1}{2\pi} \frac{W_{L+} + W_{L-}}{\rho r} \eta. \tag{12}$$

In general, the absorption coefficient is a function of laser radiation intensity and the parameters characterizing the physical state of the plasma. The absorption coefficient for the laser radiation intensity Q_L < 100 TW/cm^2 is determined mainly by the parameters of the plasma state. The absorption of laser radiation was described in the given model in a simplified approximation only accounting for the inverse bremsstrahlung mechanism. The part of the laser radiation that reaches the critical surface (where the laser radiation frequency is equal to the Langmuir frequency, i.e., $\omega = \omega_L$) is completely absorbed in this Lagrangian cell in this approximation.

In this case, the absorption coefficient of laser radiation is determined by the formula

$$\eta = 1.98.10^{-23} G \frac{\lambda^2}{T_e^{3/2}} \frac{N^2 Z^3}{\sqrt{1-\beta^2}}, \tag{13}$$

where G is the Gaunt factor; λ, cm, is the laser radiation wavelength; T_e, K, is the electron temperature; $\beta = \omega/\omega_L$ ($\omega_L = \sqrt{4\pi N_e e^2/m_e}$ is the Langmuir frequency); the condition $\beta = 1$ determines the critical value of the electron concentration $N_e = N_{ecr}$.

The critical density of plasma was found by the formula

$$\rho_{cr} = 1.88 \cdot 10^{-3} \frac{A}{Z\lambda^2}, \tag{14}$$

where A, amu, is the atomic mass of the ion; λ, μm, is the laser radiation wavelength.

If a critical concentration of electrons is obtained during propagation of laser radiation over a certain surface, the condition for complete absorption of laser radiation is imposed at this point, which means that there is no radiation flux W_{L-} in the opposite direction.

The system of equations was solved in the regions $0 \le r \le R_{Pl}(t)$, $0 \le m \le M$, $t > 0$. The boundary conditions were imposed in the following form:

on the axis of the bunch, in view of the symmetry conditions, with $m = 0$, $u(0,t) = 0$, $\frac{\partial T_e}{\partial m} = 0.$

on its outer surface, with $r = R_{Pl}(t)$, $m = M_0$, $P(M_0,t) = 0$, $\frac{\partial T_e}{\partial m} = 0..$

The model was tested with the data given in [19, 20], reporting on similar computations for laser plasma and providing the variation patterns for the plasma characteristics; these data were used as benchmark.

A carbon plasma filament is modeled in [19] with an initial concentration $N_0 = 10^{20}$ cm^{-3}, a temperature $T_{e0} = T_{i0} = 50$ eV and a radius $R_0 = 20$ μm. The pulse of a neodymium laser has a trapezoid shape with rise/fall times of 80 ps, pulse duration of 240 ps, input energy of 34 J/cm.

A cylindrical sodium plasma bunch with an initial concentration of heavy particles $N_0 = 10^{20}$ cm^{-3}, a temperature $T_{e0} = T_{i0} = 1$ eV and a radius $R_0 = 0.1$ mm was exposed in [20] to a CO_2 laser with a Gaussian pulse shape, an energy input of 6 J/cm and a characteristic time of 1 ns. In the first case, a maximum electron temperature of about 400 eV is reached in the first 100 ns, and the maximum compression is 1.1. In the second case, the equilibrium charge reaches its maximum possible value in 0.4 ns; the maximum electron temperatures are about 300 eV, and the maximum ion temperatures are about 150 eV.

Qualitatively speaking, the spatial temperature profiles in our computations appear to be more uniform. Nevertheless, the agreement between the results yielded by our code and those given in the figures in [19, 20] can be considered satisfactory.

Computational results and discussion

We have already used the model described above in our earlier computations (see [21]). We consider the results of the code for the following conditions: a cylindrical plasma bunch of sodium gas with an initial concentration of heavy particles $N_0 = 5 \cdot 10^{19}$ cm^{-3} (this corresponds to $\beta_{init} = 4.9$) and an initial radius of 0.01 cm is uniformly irradiated from the sides with a CO_2 laser; the initial temperature of sodium ions and electrons is 3 eV, the initial mean charge is defined by the Saha model.

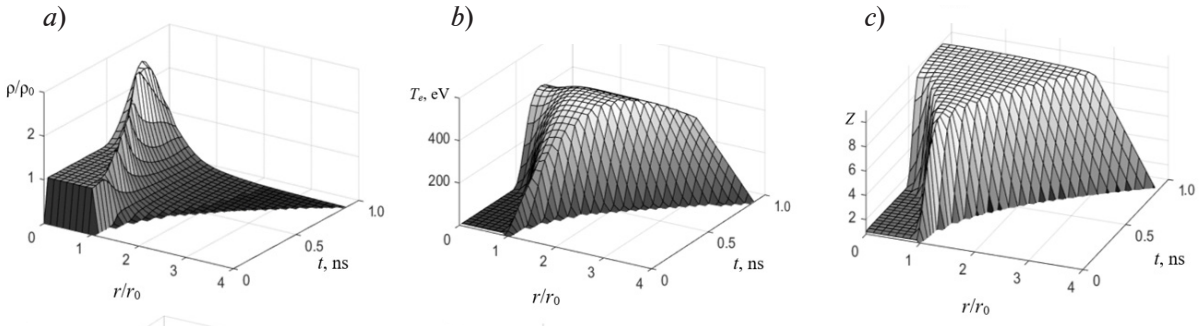

Fig. 1. Spatiotemporal distributions of density (*a*), electron temperature (*b*) and mean non-equilibrium charge (*c*) of plasma; $Q_0 = 50$ J/cm, $\beta_{init} = 4.9$

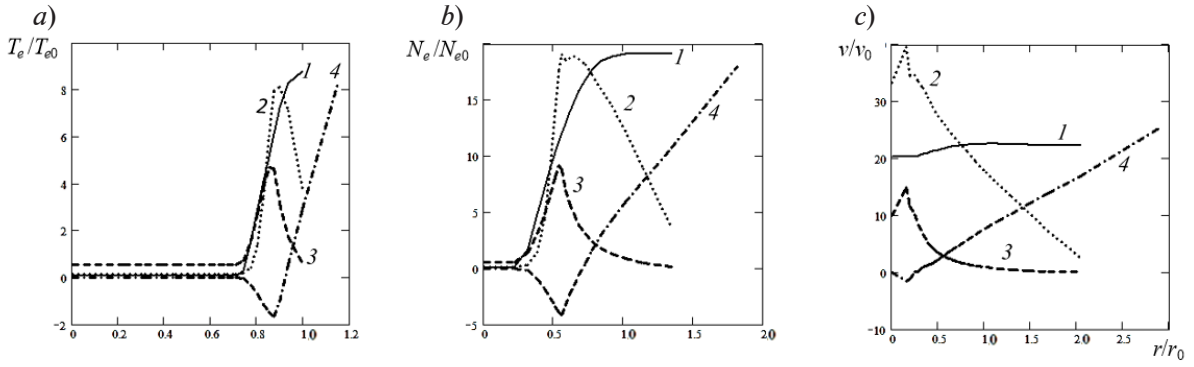

Fig. 2. Radial (over the radius of the bunch) distributions of normalized values of electron (*1*) and ion (*2*) temperature, electron concentration (*3*), and velocity (*4*) of plasma irradiated by a CO_2 laser 0.20 ns (*a*), 0.45 ns (*b*) and 0.70 ns (*c*) from the start of the exposure; $Q_0 = 50$ J/cm, $\beta_{init} = 4.9$; $T_{e0} = 20$ eV, $T_{i0} = 10$ eV, $N_e = 10^{20}$ cm^{-3}, $v_0 = 20$ km/s

The following parameters of the laser were used:
Gaussian shape of the pulse, i.e.,

$$Q(t) = Q_0 \frac{\beta_1}{\beta_0} \exp(-\beta_0{}^2 (\frac{2t}{\tau} - 1)^2);$$

$$Q_0 = 50 \text{ J/cm}, \tau = 1 \text{ ns}, \beta_1 = 0.8, \beta_0 = 2.1$$

(the parameters β_1, β_0 were selected from the conditions described in [20]).

These conditions were taken as reference in our study. Fig. 1 shows the spatiotemporal evolution of the plasma compression ratio (the ratio of its instantaneous density to the initial one), the electron temperature and the mean plasma charge. Fig. 2 also shows spatial distributions of electron and ion temperatures, electron concentrations, and plasma velocities for different times since the start of laser irradiation. Evidently, a significant part of the laser energy is absorbed in the outer layers of the bunch, so they consequently become heated strongly and expand. The plasma density at the interface with vacuum decreases during expansion, and laser radiation starts to penetrate deeper layers of the bunch, so the electron temperatures are uniformly distributed along the radius of this bunch. The electron temperature considerably deviates from the ion temperature in the cases considered, so it is reasonable to use the two-temperature approximation. The self-emission of plasma is low compared to laser radiation, and does not play any significant role in the energy transfer process.

Similar cases were observed for lower values of β_{init}, specifically, β_{init} = 1.9 and 0.8 (in the second case, the density is below critical). The key computational results are given in the table: the maximum temperature, compression ratio and mean charge achievable during irradiation with the laser pulse. Interestingly, a local peak is observed on the dependence of the maximum mean charge on the initial plasma density. Fig. 3 shows the spatiotemporal distributions of the mean non-equilibrium plasma charge for the cases of β_{init} = 1.9 and 0.8. Apparently, virtually no outer layers with higher characteristics appear to evolve at $\beta_{init} < 1$; these layers are concentrated towards the bunch axis (their presence can also be seen in Fig. 1).

Aside from varying the initial concentration, the energy input was also varied in the range of 50–80 J/cm for the reference case β_{init} = 4.9 (see Table). We established that an energy input of 70 J/cm is sufficient to achieve nearly complete ionization of the plasma bunch under these initial conditions. Similarly, the minimum energy inputs necessary to obtain a particular plasma composition can be found for outer initial/external conditions.

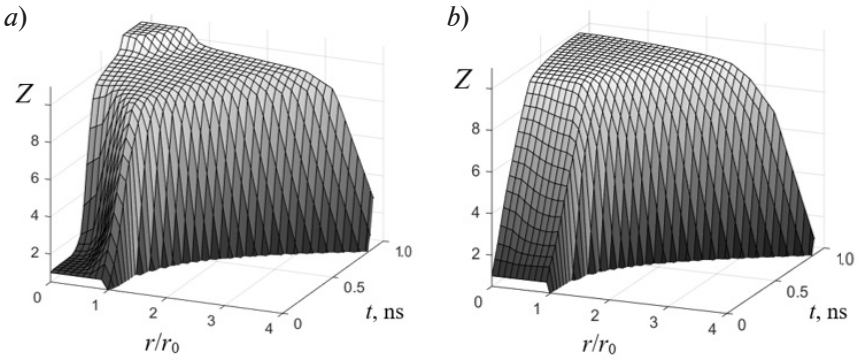

Fig. 3. Spatiotemporal distributions of the average non-equilibrium plasma charge for the initial concentrations of heavy particles β_{init} = 1.9 and 0.8

Table

Calculated maximum values of the key plasma parameters achievable during the laser pulse

E, J/cm	β_{init}	Z_{max}	$(T_e)_{max}$, eV	$(\rho/\rho_0)_{max}$
50	4.9	9.85	455	2.79
	1.9	11.00	953	1.49
	0.8	9.85	811	1.01
60	4.9	10.00	530	2.59
70		11.00	606	2.47
80		11.00	676	2.38

Notations: E is the energy input, β_{init} is the initial concentration of heavy particles, Z_{max} is the mean ion charge, $(T_e)_{max}$ is the temperature of electrons, $(p/p_0)_{max}$ is the plasma compression ratio

Conclusion

Effective amplification of short-wave radiation in multicharged ion plasma can be achieved through obtaining a specific charge composition of the plasma (even though this is a necessary but insufficient condition). We present the calculations confirming that the most favorable conditions for obtaining a certain plasma charge can be established.

The electromagnetic fluxes of the CO_2 laser used in the calculations, irradiating the lateral surface of the medium, lie in the range that is well mastered experimentally: the laser generation intensity W does not exceed 100 TW/cm^2. The dynamics of plasma behavior is illustrated by spatiotemporal graphs constructed for the main characteristics of cylindrical plasma bunches. Cases with different initial densities are considered; we found that there is a local peak on the dependence of the maximum mean charge reached on the initial plasma density. We particularly focused on the average plasma charge in the calculations. The cases when the average charge reaches $(9-11)\times1.6\cdot10^{-19}$ C are considered, making it possible to generate plasma consisting of hydrogen and helium-like ions of the medium with electron transitions at wavelengths $\lambda \leq 10$ nm.

We plan to apply the code developed to analyzing the time profiling of laser pulses and the initial non-uniform distribution of plasma density to subsequently solve the problems related to generating plasma with the necessary non-equilibrium ionic composition.

REFERENCES

1. **Elton R. C.,** X-ray lasers, Academic Press inc., New York, 1990.

2. **Boyko V. A., Bunkin V. F., Derzhiyev V. I., Yakovlenko S. I.,** Vozmozhnosti usileniya ultrafioletovogo i myagkogo rentgenovskogo izlucheniya na perekhodakh mnogozaryadnykh ionov v rekombiniruyushchey plazme [Amplification potentials for ultraviolet and soft X-ray radiation based on multicharged-ion's transitions in the recombining plasma], Bulletin of the Academy of Sciences of the USSR. Physical Series. 47 (10) (1983) 1880–1897 (in Russian).

3. **Nilsen J.** X-ray lasers: The evolution from Star Wars to the table-top, Proc. SPIE. 2021. Vol. 11886. Intern. Conf. on X-Ray Lasers. 2020. P. 1188604 (8 July 2021).

4. **Suckewer S., Jaegle P.,** X-ray laser: past, present, and future, Laser Phys. Lett. 6 (6) (2009) 411–436.

5. **Kördel M., Dehlinger A., Seim C., et al.,** Laboratory water-window X-ray microscopy, Optica. 7 (6) (2020) 658–674.

6. **Do M., Isaacson S. A., McDermott G., et al.,** Imaging and characterizing cells using tomography, Arch. Biochem. Biophys. 581 (1 September) (2015) 111–121.

7. **Harth A., Guo Ch., Cheng Y.-Ch., et al.,** Compact 200 kHz HHG source riven by a few-cycle OPCPA, J. Opt. 20 (1) (2018) 014007.

8. **Dunne M.,** X-ray free-electron lasers light up materials science, Nat. Rev. Mat. 3 (16 August) (2018) 290–292.

9. **Namba S., John C., Morishita T., et al.,** Observation of gain coefficients of 15.47 nm Li-like Al soft X-ray laser in a recombining plasma pumped by a compact YAG laser, High Energy Density Phys. 36 (August) (2020) 100790.

10. **Wachulak P., Torrisi A., Nawaz M. F., et al.,** A compact "Water Window" microscope with 60 nm spatial resolution for applications in biology and nanotechnology, Microsc. Microanal. 21 (5) (2015) 1214–1223.

11. **Rocca J. J.,** Table-top soft X-ray lasers, Rev. Sci. Instr. 70 (10) 3799–3827.

12. **Barnwal S., Nigam S., Aneesh K., et al.,** Exploring X-ray lasing in nitrogen pinch plasma at very high and fast discharge current excitation, Appl. Phys. B. 123 (6) (2017) 178.

13. **Kuzenov V. V., Lebo A. I., Lebo I. G., Ryzhkov S. V.,** Physical and mathematical models and methods of calculation for interaction of intensive laser and plasma pulses with condensed and gas environments, 2nd Ed., Published by MGTU named after N. E. Bauman, Moscow, 2017 (in Russian).

14. **Basko M. M., Tsygvintsev I. P.,** A hybrid model of laser energy deposition for multi-dimensional simulations of plasmas and metals, Comput. Phys. Commun. 214 (May) (2017) 59–70.

15. **Sizyuk V., Hassanein A., Morozov V., et al.,** Numerical simulation of laser-produced plasma devices for EUV lithography using the heights integrated model, Numer. Heat Transf. A. 49 (3) (2006) 215–236.

16. **Kim D. A., Vichev I. Y.,** Modeling of liquid tin target by laser pulse, Keldysh Institute Preprints, Moscow. (122) (2017) 1–19 (in Russian).

17. **Sedov M. V., Platonov K. Yu., Andreev A. A.,** Simulation of the generation of K_α-radiation upon the interaction of intense laser radiation with a solid target, Bull. St. Petersburg State Univ. Phys. & Chem. 4 (62) (2017) 23–33.

18. **Afanasiev Yu. V., Gamaliy E. G., Rozanov V. B.,** Osnovnyye uravneniya dinamiki i kinetiki lazernoy plazmy [Basic equations of dynamics and kinetics of a laser plasma], Trudy FIAN. Teoriya nagreva i szhatiya nizkoentropiynykh termoyadernykh misheney [LPI Transactions: The theory of heating and compression of low-entropic thermonuclear targets]. 134 (1982) 10–31 (in Russian).

19. **Bakhvalov N. S., Borovskii A. V., Korobkin V. V., et al.,** Heating and non-equilibrium thermal ionization of a plasma by means of a short laser pulse, Preprint of General Physics Institute of the Academy of Sciences of the USSR, Moscow (166) (1986) 1–22 (in Russian).

20. **Babarskov E. V., Derzhiev V. I., Evstigneev V. V., Yakovlenko S. I.,** Analysis of the formation of the active medium at $\lambda = 15.5$ nm plasma laser pumped by a CO_2 laser, Soviet Journal of Quantum Electronics. 11 (10) (1981) 1306–1310.

21. **Kalinin N. V., Timshina M. V.,** Dinamika i neravnovesnyy sostav plazmy mnogozaryadnykh ionov, sozdavayemoy pri vzaimodeystvii moshchnogo lazernogo izlucheniya s tsilindricheskoy plazmennoy mishenyu [Dynamics and non-equilibrium composition of multicharged ion plasma produced in interaction between high-power laser radiation and a cylindrical plasma's target], Techn. Phys. Lett. 48 (6) (2022) in print.

СПИСОК ЛИТЕРАТУРЫ

1. **Элтон Р.** Рентгеновские лазеры: Пер. с англ. М.: Мир, 1994. 335 с.

2. **Бойко В. А., Бункин В. Ф., Держиев В. И., Яковленко С. И.** Возможности усиления ультрафиолетового и мягкого рентгеновского излучения на переходах многозарядных ионов в рекомбинирующей плазме // Известия АН СССР. Серия физическая. 1983. Т. 47. № 10. С. 1880–1897.

3. **Nilsen J.** X-ray lasers: The evolution from Star Wars to the table-top // Proceedings of SPIE. 2021. Vol. 11886. International Conference on X-Ray Lasers. 2020. P. 1188604 (8 July 2021).

4. **Suckewer S., Jaegle P.** X-ray laser: past, present, and future // Laser Physics Letters. 2009. Vol. 6. No. 6. Pp. 411–436.

5. **Kördel M., Dehlinger A., Seim C., Vogt U., Fogelqvist E., Sellberg J. A., Stiel H., Hertz H. M.** Laboratory water-window X-ray microscopy // Optica. 2020. Vol. 7. No. 6. Pp. 658–674.

6. **Do M., Isaacson S. A., McDermott G., Le Gros M. A., Larabell C. A.** Imaging and characterizing cells using tomography // Archives of Biochemistry and Biophysics. 2015. Vol. 581. 1 September. Pp. 111–121.

7. **Harth A., Guo Ch., Cheng Y.-Ch., et al.** Compact 200 kHz HHG source riven by a few-cycle OPCPA // Journal of Optics. 2018. Vol. 20. No. 1. P. 014007.

8. **Dunne M.** X-ray free-electron lasers light up materials science // Nature Reviews Materials. 2018. Vol. 3. 16 August. Pp. 290–292.

9. **Namba S., John C., Morishita T., Kubo N., Kishimoto M., Hasegawa N., Nishikino M.** Observation of gain coefficients of 15.47 nm Li-like Al soft X-ray laser in a recombining plasma pumped by a compact YAG laser // High Energy Density Physics. 2020. Vol. 36. August. P. 100790.

10. **Wachulak P., Torrisi A., Nawaz M. F., et al.** A compact "Water Window" microscope with 60 nm spatial resolution for applications in biology and nanotechnology // Microscopy and Microanalysis. 2015. Vol. 21. No. 5. Pp. 1214–1223.

11. **Rocca J. J.** Table-top soft X-ray lasers // Review of Scientific Instruments. 1999. Vol. 70. No. 10. Pp. 3799–3827.

12. **Barnwal S., Nigam S., Aneesh K., Prasad Y. B. S. R., Sharma M. L., Tripathi P. K., Joshi A. S., Naik P. A., Vora H. S., Gupta P. D.** Exploring X-ray lasing in nitrogen pinch plasma at very high and fast discharge current excitation // Applied Physics B. 2017. Vol. 123. No. 6. P. 178.

13. **Кузенов В. В., Лебо А. И., Лебо И. Г., Рыжков С. В.** Физико-математические модели и методы расчета воздействия мощных лазерных и плазменных импульсов на конденсированные и лазерные среды. М.: Изд-во МГТУ им. Н. Э. Баумана, 2017. 326 с.

14. **Basko M. M., Tsygvintsev I. P.** A hybrid model of laser energy deposition for multi-dimensional simulations of plasmas and metals // Computer Physics Communications. 2017. Vol. 214. May. Pp. 59–70.

15. **Sizyuk V., Hassanein A., Morozov V., Tolkach V., Sizyuk T., Rice B.** Numerical simulation of laser-produced plasma devices for EUV lithography using the heights integrated model // Numerical Heat Transfer. Part A. 2006. Vol. 49. No. 3. Pp. 215–236.

16. **Ким Д. А., Вичев И. Ю.** Моделирование деформации жидкой оловянной капли в результате воздействия лазерного импульса. Препринты ИПМ им. М. В. Келдыша. № 122. М.: Изд. Института прикладной математики им. М. В. Келдыша РАН, 2017. 19 с.

17. **Sedov M. V., Platonov K. Yu., Andreev A. A.** Simulation of the generation of K_α-radiation upon the interaction of intense laser radiation with a solid target // Bulletin of St. Petersburg State University. Physics and Chemistry. 2017. Vol. 4. No. 62. Pp. 23–33.

18. **Афанасьев Ю. В., Гамалий Е. Г., Розанов В. Б.** Основные уравнения динамики и кинетики лазерной плазмы // Труды ФИАН. Т. 134. Теория нагрева и сжатия низкоэнтропийных термоядерных мишеней (Сборник статей). М.: Наука, 1982. С. 10 – 31.

19. **Бахвалов Н. С., Боровский А. В., Коробкин В. В., Чижонков Е. В., Эглит М. Э.** Нагрев и неравновесная тепловая ионизация плазмы коротким лазерным импульсом. Препринт ИОФ АН СССР. № 166. М.: Изд. Института общей физики Академии наук СССР, 1986. 21 с.

20. **Бабарсков Е. В., Держиев В. И., Евстигнеев В. В., Яковленко С. И.** Анализ формирования активной среды плазменного лазера на $\lambda = 15{,}5$ нм с помощью CO_2-лазера // Квантовая электроника. 1981. Т. 8. № 10. С. 2136–2144.

21. **Калинин Н. В., Тимшина М. В.** Динамика и неравновесный состав плазмы многозарядных ионов, создаваемой при взаимодействии мощного лазерного излучения с цилиндрической плазменной мишенью // Письма в Журнал технической физики. 2022. Т. 48. № 6. С. 11–15.

THE AUTHORS

TIMSHINA Mariia V.
Ioffe Institute of the Russian Academy of Sciences
26 Polytekhnicheskaya St., St. Petersburg, 194021, Russia
mariyatimshina@yandex.ru
ORCID: 0000-0002-3868-3797

KALININ Nikolai V.
Peter the Great St. Petersburg Polytechnic University
29 Politechnicheskaya St., St. Petersburg, 195251, Russia
nvkalinin@rambler.ru

СВЕДЕНИЯ ОБ АВТОРАХ

ТИМШИНА Мария Викторовна – *младший научный сотрудник лаборатории квантоворазмерных гетеростуктур Физико-технического института имени А. Ф. Иоффе Российской академии наук.*
194021, Россия, г. Санкт-Петербург, Политехническая ул., 26
mariyatimshina@yandex.ru
ORCID: 0000-0002-3868-3797

Калинин Николай Валентинович – *доктор физико-математических наук, профессор кафедры высшей математики Санкт-Петербургского политехнического университета Петра Великого.*
195251, Россия, г. Санкт-Петербург, Политехническая ул., 29
nvkalinin@rambler.ru

Received 14.06.2022. Approved after reviewing 18.08.2022. Accepted 18.08.2022.
Статья поступила в редакцию 14.06.2022. Одобрена после рецензирования 18.08.2022. Принята 18.08.2022.